Molecular Therapy
Methods & Clinical Development
Original Article

Preclinical efficacy of a modified gamma-globin lentivirus gene therapy in Berkeley sickle cell anemia mice and human xenograft models

Archana Shrestha,[1,2,5] Devin M. Pillis,[1,6] Sydney Felker,[1,7] Mengna Chi,[1] Kimberly Wagner,[1] Oluwabukola T. Gbotosho,[1,8] Joseph Sieling,[2,9] Mohammad Shadid,[2] and Punam Malik[1,3,4]

[1]Division of Experimental Hematology and Cancer Biology, Cincinnati Children's Hospital Medical Center (CCHMC), Cincinnati, OH 45229, USA; [2]Aruvant Sciences, New York, NY 10036, USA; [3]Division of Hematology, Cincinnati Children's Hospital Medical Center, Cincinnati, OH 45229, USA; [4]Department of Pediatrics, University of Cincinnati, Cincinnati, OH 45229, USA

We previously showed correction of sickle cell anemia (SCA) in mice utilizing a lentiviral vector (LV) expressing human γ-globin. Herein, we made a G16D mutation in the γ-globin gene to generate the G16D mutation (GbG^{M}) LV to increase fetal hemoglobin formation. We also generated an insulated version of this LV, GbG^{MI}, inserting a 36-bp insulator from the Foamy virus in the long terminal repeats of the LV. Preclinical batches of GbG^{M} and GbG^{MI} LV showed both were highly efficacious in correcting SCA in mice, with sustained gene transfer in primary transplanted SCA mice and high hematopoietic stem cell (HSC) transduction in colony-forming unit-spleen in secondary transplanted mice. CRISPR-mediated targeting of the proviruses into the LMO2 proto-oncogene showed remarkably reduced LMO2 activation by both insulated and uninsulated LV, compared to the SFFV γ-RV vector targeted to the same locus. We therefore used the GbG^{M} LV to perform preclinical human $CD34^{+}$ gene transfer. We assessed gene transfer and engraftment of human HSCs in two immunocompromised mouse models: persistent stable GbG^{M}-transduced cell engraftment was comparable to that of untransduced cells with no detrimental effects on hematopoiesis up to 20 weeks post transplant. These robust preclinical studies in mouse and human HSCs allowed its translation into a clinical trial.

INTRODUCTION

Sickle cell anemia (SCA) is a devastating hereditary disorder due to a change in the sixth codon of the human β-globin (HBB) gene that results in the replacement of glutamic acid by valine in hemoglobin, resulting in formation of sickle hemoglobin (HbS). HbS polymerizes upon deoxygenation,[1,2] changing the shape of the normally round red blood cells (RBCs) to sickle shaped cells.[1,3,4] Sickle RBCs are rigid and poorly deformable and clog microcirculation, causing substantial organ damage and critical painful episodes, severely affecting the quality of life and are a significant impact on the healthcare system.[5,6] The molecular diagnosis of SCA was discovered seven decades ago,[2,7] yet curative options remain limited. Current therapeutic approaches for SCA involve management of symptoms, chronic transfusions, or life-long use of hydroxyurea, which reactivates endogenous fetal hemoglobin (HbF). However, compliance with daily life-long drug therapy and frequent monitoring of blood counts and costs are barriers to effective therapy. Additionally, a portion of patients do not respond to hydroxyurea.[8] Allogeneic hematopoietic stem cell transplantation (allo-HSCT) offers a cure for SCA, but its use is limited by the availability of well-matched donors, risk of graft rejection, and risk of graft-versus-host disease.[9,10] Genetic modification followed by autologous HSCT, in which patients are their own hematopoietic stem cell (HSC) donors for gene modification, provides a promising alternative strategy for the permanent cure of SCA,[7,11–13] circumventing the limitations of donor availability and immune side effects associated with allo-HSCT.

Lentiviral vectors (LVs) have now been in clinical trials for over 15 years and have resulted in the cure of several inherited blood diseases such as severe combined immunodeficiency, chronic granulomatous disease, adrenoleukodystrophy (ALD) (Skysona), Wiskott-Aldrich syndrome, SCA, and β-thalassemia (Zynteglo).[14–22] We have previously shown that a human gamma-globin LV, $G^{b}G$, which carries

Received 24 July 2024; accepted 18 February 2025;
https://doi.org/10.1016/j.omtm.2025.101439.

[5]Present address: Pharmaron, Inc., Exton, PA 19341, USA

[6]Present address: MedStar Franklin Square Medical Center, Baltimore, MD 21237, USA

[7]Present address: College of Medicine, University of Cincinnati, Cincinnati, OH, USA

[8]Present address: Department of Neurology and Rehabilitation Medicine, University of Cincinnati, Cincinnati, OH, USA

[9]Present address: Legend Biotech, Somerset, NJ 08873, USA

Correspondence: Punam Malik, Division of Experimental Hematology and Cancer Biology, Cincinnati Children's Hospital Medical Center, Cincinnati, OH 45229, USA.
E-mail: punam.malik@cchmc.org

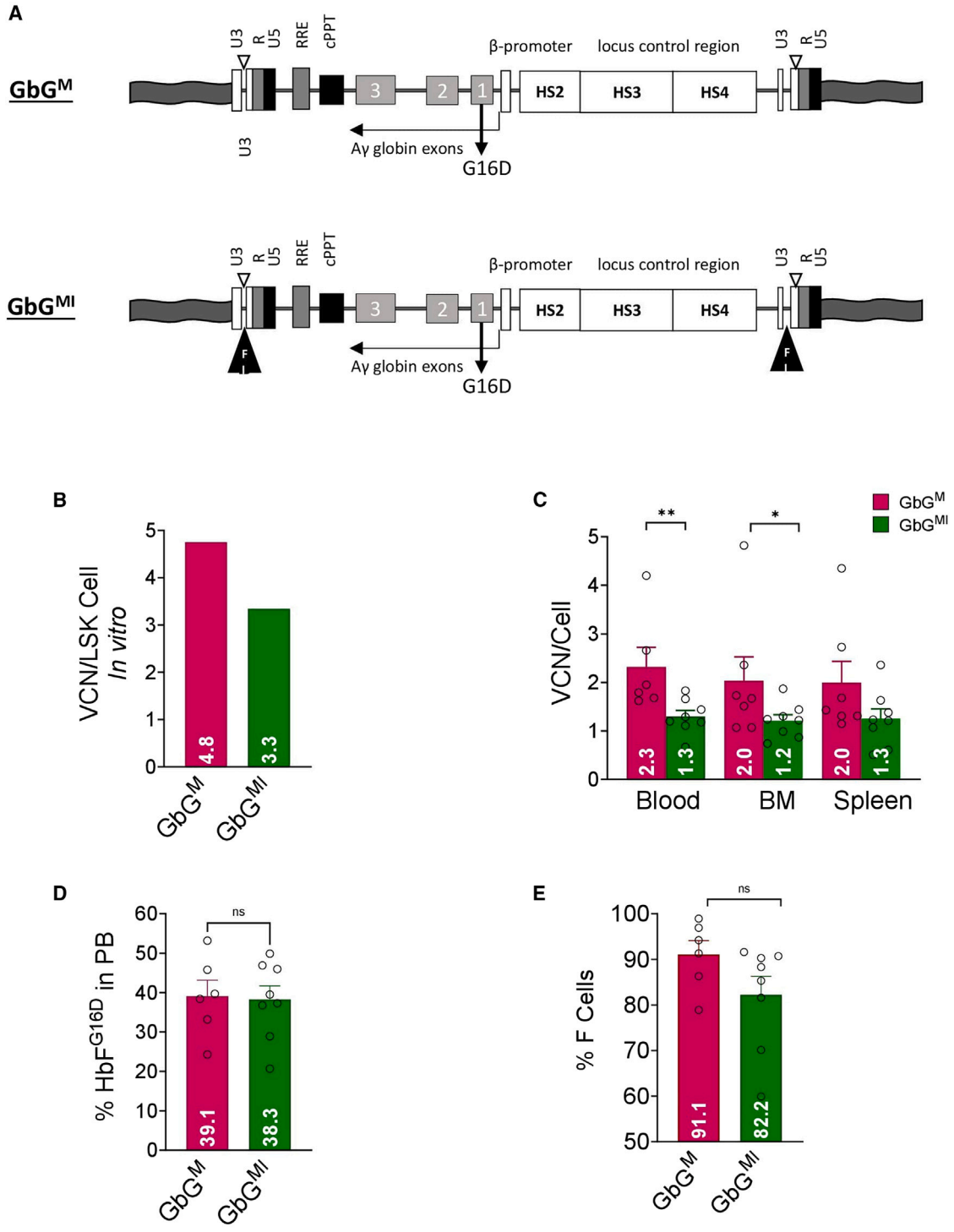

Figure 1. Effects of GbG^{M} and GbG^{MI} Lentiviral vector (LV) vector gene transfer in primary transplanted SS mice

(A) Structure of a modified γ-globin gene (GbG^{M}) carrying self-inactivating lentiviral vector GbG^{M} (without the Foamy virus insulator element [top panel]) and (with the Foamy virus insulator [bottom panel, triangle labeled as FI]) GbG^{MI} in its proviral form. A point mutation was created in exon 1 γ-globin gene to change glycine, G, at the 16th codon to aspartic acid, D. (B) Bone marrow (BM)-derived stem and progenitor cells (lineage^{-} Sca1^{+} cKit^{+} [LSK]) of donor SS mice were transduced with GbG^{M} or GbG^{MI} LV and VCN in the LSK cells post gene transfer were transplanted into sub-lethally irradiated SS recipient mice. (C) The vector copy number (VCN) in PB, BM, and spleen (analyzed via qPCR)

(legend continued on next page)

the human Aγ-globin exons and β-globin non-coding regions and is driven by the β-globin gene promoter and the locus control region's (LCR) hypersensitive sites 2, 3, and 4 enhancers, expresses therapeutic levels of HbF to correct SCA in a humanized sickle mouse model with reduced intensity conditioning.[22] Herein, we mutated the G^bG LV, termed GbG^M, to achieve a competitive advantage of the γ^{G16D}-globin over β^{Sickle} globin chains to form the HbF tetramer. The GbG^M resulted in a 1.5–2× increase in HbF expression and therefore enhanced the anti-sickling efficacy more than the base G^bG LV (Grimley et al., personal communication).

Despite the fact that erythroid-lineage-specific enhancers in self-inactivating LV have shown an excellent safety profile in other gene therapy trials for SCA and β-thalassemia, the LCR enhancer has been shown to have weak activity in HSCs, and hence there may be a small risk of vector-mediated genotoxicity.[24–26] Chromatin insulators in LV can add an additional safety feature by blocking enhancers located within the integrating vector genome.[27] However, prior chromatin insulators have generally been large, recombined, or have lowered vector titers. We discovered a small potent enhancer-blocking insulator sequence in Foamy virus vectors that does not affect vector titers[28] and inserted this in the 3′ long terminal repeat (LTR) of GbG^M to generate the GbG^{MI} LV so that the insulator is copied over to the 5′ LTR in the provirus (integrated vector) to assess if it further improves safety.

Herein, we performed preclinical studies of GbG^M and GbG^{MI} LV to evaluate and compare their efficacy in correcting SCA phenotype in a Berkeley sickle mouse [$Tg(Hu\text{-}miniLCR\alpha1^G\gamma^A\gamma\delta\beta^S)$ $Hba^{0/0}$ $Hbb^{0/0}$][29] (SS) model and a secondary transplant colony-forming unit (CFU)-spleen (CFU-S) assay. We also evaluated the enhancer-blocking ability of GbG^M and GbG^{MI} LV by knocking in the provirus forms within the LMO2 proto-oncogene. We found both vectors were similarly efficacious at correcting SCA and had a remarkably better safety profile than retroviral (RV) vectors, which have been known to increase LMO2 expression, resulting in leukemia. We then evaluated long-term engraftment and biodistribution of the GbG^M-transduced human $CD34^+$ cells from healthy donors after xenotransplantation in NOD.Cg-$Prkdc^{scid}$ $Il2rg^{tm1Wjl}$/SzJ (NSG) and NOD.Cg-Kit^{W-41J} Tyr^+ $Prkdc^{scid}$ $Il2rg^{tm1Wjl}$/ThomJ (NBSGW)[30] mouse models as preclinical studies to support the phase 1/2 clinical development of GbG^M gene therapy for SCA (ClinicalTrials.gov: NCT02186418). After selecting the GbG^M vector to proceed to the clinic and to include in the Investigational New Drug (IND) submission, we conducted a safety assessment of the vector in healthy mice.[31]

RESULTS

Effective gene transfer in murine hematopoietic stem and progenitor cells *in vitro* and *in vivo*

We modified our previously published GbG LV that expresses high level of HbF and corrects SCA in mice following reduced intensity conditioning.[23] We improved this LV by generating the GbG^M LV, which carries a point mutation (G16D in the γ-globin gene) (Figure 1A), to increase HbF tetramer formation by altering the γ-globin electrostatic charge as compared to native γ-globin (data under review as a separate manuscript). Additionally, for further safety of GbG^M, a 36-bp sequence of the Foamy virus insulator was added to the 3′ LTR to generate the GbG^{MI} LV to potentially block activation of the surrounding genes by the β-globin LCR enhancer in the LV (Figure 1A). The LV concentrated titers were very similar between GbG^M and GbG^{MI} LV (Figure S1A).

The pathophysiology of SS mice closely resembles severe human SCA and thus SS mice were used as both donor and recipients for the study. Preliminary pilot experiments were performed to optimize a vector multiplicity of infection (MOI) that results in a high transduction efficiency. Based on the results, an MOI of 25 was chosen for targeting vector copy number (VCN) of 2–5 copies per cell. $Lineage^-$ $Sca\text{-}1^+$ $cKit^+$ (LSK) hematopoietic stem and progenitor cells (HSPCs) were sorted from SS mouse bone marrow (BM), transduced with GbG^M or GbG^{MI} vector, or sham transduced (mock), followed by transplantation into sub-lethally irradiated recipient SS mice. Transplanted mice were followed for 24 weeks or more, and the effects on hematological parameters at different time points were analyzed (Figure S1B). A portion of transduced LSK cells were maintained in culture for 14 days for VCN analysis of the cells that were transplanted. The GbG^M-transduced HSPCs showed an average VCN of 4.8 per cell, while GbG^{MI}-transduced HSPCs had an average VCN of 3.3, indicating high level of gene transfer *in vitro* (Figure 1B).

Following transplant, all mice were monitored daily and weighed weekly. Animals had minimal weight fluctuations and showed no remarkable weight loss in the peri-transplant period. There were four animal deaths observed during the study (three in the mock group and one in the GbG^M group in the period of 9–18 weeks), which were likely related to sickle cell disease or procedure-related mortality (as is routinely seen in SS mice). Peripheral blood (PB) analysis of mice transplanted with GbG^M- and GbG^{MI}-transduced HSPCs at 6–8 weeks post transplant showed VCN similar to the *in vitro* VCN in the transduced LSK cells (Figures S1C and S1B). Human globin subtype analysis via capillary zone electrophoresis (CZE) of GbG^M mice and GbG^{MI} mice showed ∼39%–48% HbF^{G16D} expression at 6–8 weeks (Figure S1D).

Sustained engraftment and phenotypic correction in primary transplant recipient SS mice

To evaluate the long-term engraftment of gene-marked donor cells, recipient GbG^M, GbG^{MI}, and mock SS mice were terminally bled and sacrificed at 24 weeks post transplantation. Analysis of VCN in PB showed an average of 2.3 copies per cell in GbG^M mice and

at 24 weeks after transplant of GbG^M or GbG^{MI} LSK cells in primary recipients. (D) Modified fetal hemoglobin (HbF^{G16D}) production and (E) the percentage of cells containing HbF (F cells) in GbG^M and GbG^{MI} mice at 24 weeks are shown; data presented as mean ± SEM. Each symbol in the bar graph represents an individual animal. (C, D, and E) Statistics: unpaired Student's t test. ns, not significant; $^*p < 0.05$, $^{**}p < 0.01$.

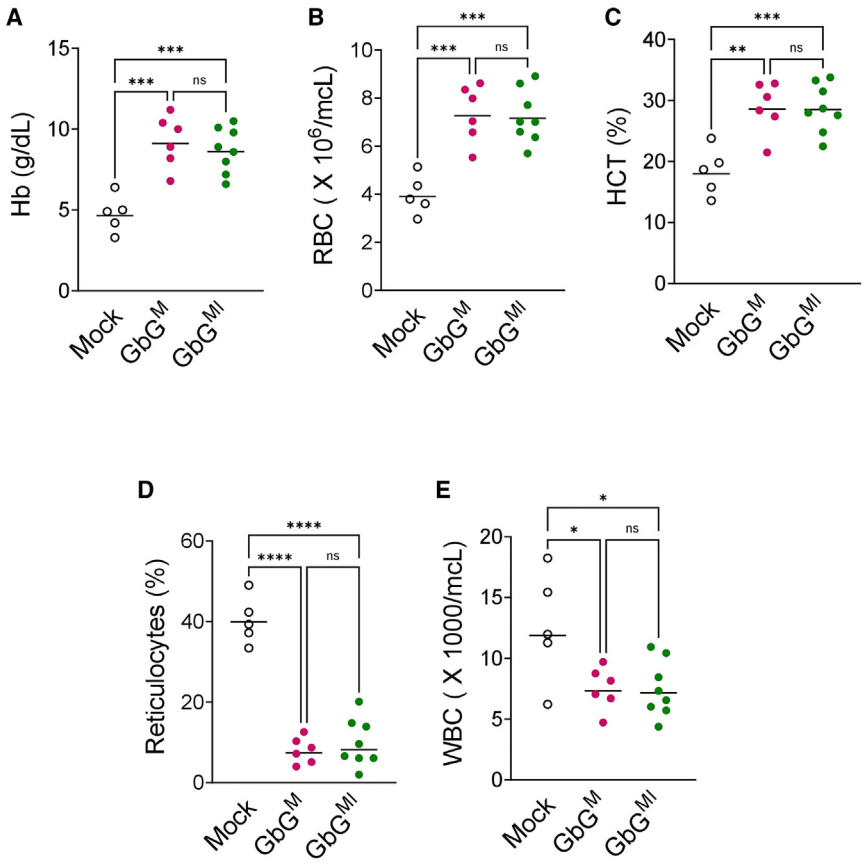

Figure 2. Hematological parameters after GbG^{M} and GbG^{MI} LV gene transfer in primary transplanted SS mice

Hematological parameters of mock, GbG^{M}, and GbG^{MI} mice at 24 weeks post primary transplant. (A) Hemoglobin (Hb), (B) red blood cell (RBC) count, (C) hematocrit (HCT), (D) reticulocytes, and (E) white blood cell (WBC) count in the PB. (A–E) n = 5 mock SS mice, n = 6 GbG^{M} SS mice, and n = 8 GbG^{MI} SS mice. Geometric mean was marked in each scatterplot. Each symbol represents an individual animal. Statistics: one-way ANOVA. ns, not significant; *p < 0.05, **p < 0.01, ***p < 0.001, ****p < 0.0001. Note: one GbG^{M} mouse was excluded from terminal CBC analysis due to a clot in the PB.

1.3 copies per cell in GbG^{MI} mice, which were clinically relevant VCNs (1–3 copies per cell is commonly achieved in the clinical setting) (Figure 1C). Similar levels of VCN were also observed in other hematopoietic organs such as BM and spleen (Figure 1C) at 24 weeks post transplantation, demonstrating gene marking in a long-term repopulating HSC. The expression of anti-sickling globin HbF^{G16D} showed similar level of HbF^{G16D} in GbG^{M} and GbG^{MI} mice (Figures 1D and S2E). An F cell analysis was also performed to assess the percentage of HbF containing RBCs. We observed greater than 80% F cells in the PB of GbG^{M} and GbG^{MI} animals (Figure 1E). In addition, HbF containing erythroid cells were also detected in BM and spleen ranging from 52% to 54% in GbG^{M} mice and 44% to 47% in GbG^{MI} mice (Figure S2A).

A high F cell percentage was associated with sustained hematological correction in both GbG^{M} and GbG^{MI} mice until the end of the study. Analysis of hematological indices in recipient SS mice showed significant reduction in anemia with more than an average of 4 g/dL increase in Hb compared to the mock mice. The Hb rose to 9.2 ± 0.7 g/dL (mean ± standard error of mean [SEM]) in GbG^{M} mice and 8.7 ± 0.5 g/dL in GbG^{MI} mice, whereas mock mice had Hb of 4.8 ± 0.5 g/dL (Figure 2A). Similarly, RBC counts and hematocrit (HCT) fractions were significantly increased in both GbG^{M} and GbG^{MI} mice when compared to mock mice, suggesting higher RBC survival in the mice receiving vector-transduced cells (Figures 2B and 2C). Reticulocytosis was also markedly reduced from 40.2% ± 2.6% in mock mice down to 7.9% ± 1.3% and 9.9% ± 2.1% in GbG^{M} and GbG^{MI} mice, respectively (Figure 2D).

Leukocytosis is reflective of chronic inflammation in SCA.[32] Indeed, the SS mice transplanted with mock-transduced HSPCs presented with increased leukocyte counts, while, in both GbG^{M} and GbG^{MI} mice, leukocytosis was significantly improved (Figure 2E).

Improved RBC function from GbG^{M}- and GbG^{MI}-transduced HSPCs in SS mice

In order to assess functional correction with GbG^{M} and GbG^{MI} LV, we evaluated the sickling kinetics and RBC membrane deformability in the PB of SS recipient mice at 24 weeks after transplantation by ektacytometry using Lorrca Oxygenscan.[33] During ektacytometry, RBCs' ability to deform/elongate is measured with increasing shear stress under normoxia. Sickle RBCs are rigid and less deformable than normal RBCs due to membrane damage sustained from sickling and unsickling.[34] Normal or wild-type (WT) RBCs elongate easily at low shear stress, while sickle RBCs resist elongation even at higher shear stress. In both GbG^{M} and GbG^{MI} mice, RBC deformability was markedly improved, approaching that of normal (C57BL/6J) WT RBCs when compared to mock mice before and after one cycle of deoxygenation/reoxygenation (Figures 3A and 3B). RBC sickling kinetics were measured by subjecting PB RBCs to controlled deoxygenation from normoxic to hypoxic levels of oxygen pressure (pO_2 < 15 mm Hg) followed by reoxygenation back to normoxic levels and measuring RBC deformability (elongation index [EI]) at a fixed shear stress.[33] EI_{max} (highest EI at ambient pO_2), point of sickling (PoS: pO_2 when the EI drops to 95% of the EI_{max}), and EI_{min} (minimum EI after deoxygenation) were measured. Blood analysis at 24 weeks post transplant showed both GbG^{M} and GbG^{MI} animals with

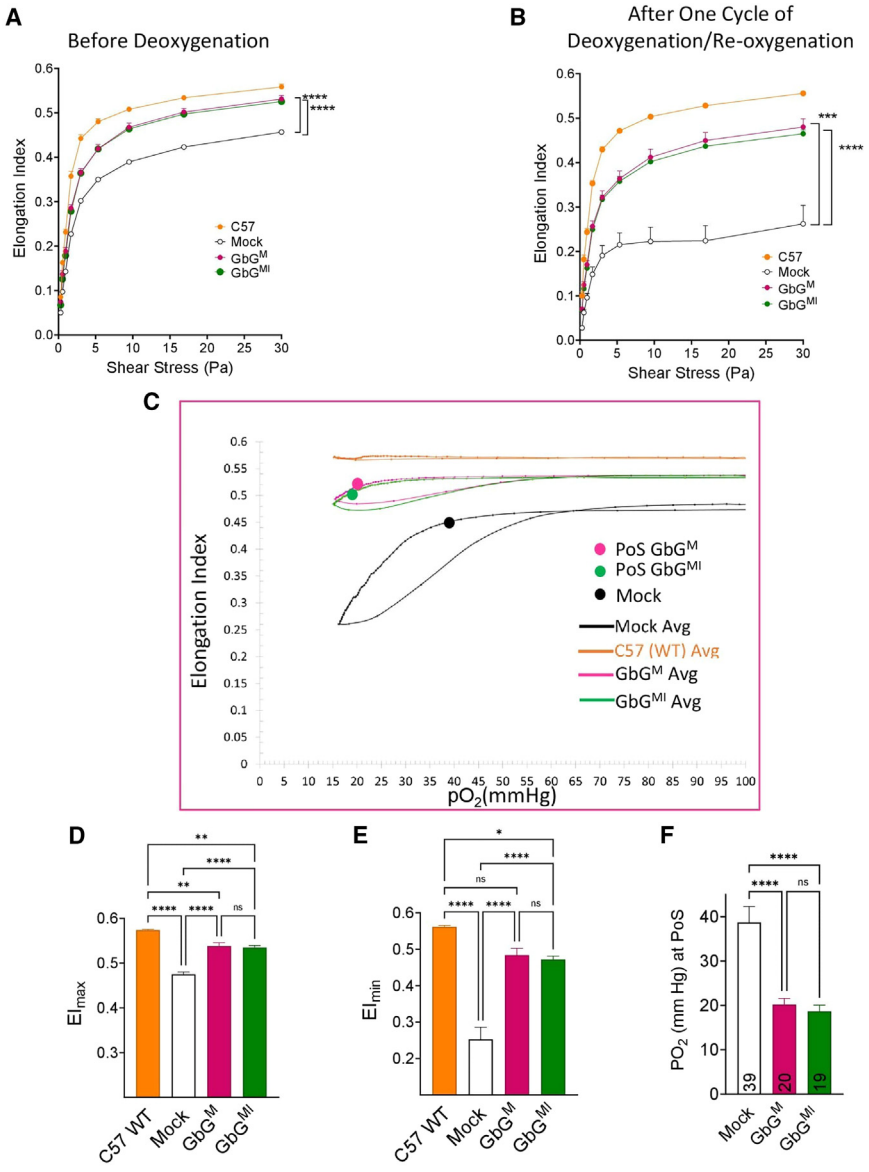

Figure 3. RBC membrane deformability and sickling kinetics in GbG^{M} and GbG^{MI} mice as compared to mock mice

(A and B) RBC membrane deformability (elongation index [EI]) was measured at increasing shear stress (between 0.3 and 30 Pa) under ambient pO_2 for GbG^{M}, GbG^{MI}, and mock mice along with a WT C57 mouse as control (A) before deoxygenation and (B) after one round of deoxygenation and reoxygenation. Data presented as mean ± SEM. (A and B) Statistics: two-way ANOVA; $^{***}p < 0.001$, $^{****}p < 0.0001$. (C–F) Oxygen scan ektacytometry curves on RBCs from GbG^{M}, GbG^{MI}, and mock mice that were subjected to controlled deoxygenation from pO_2 of 150 mm Hg to 15 mmHg, followed by reoxygenation. EI_{max} is the highest deformability; the point of sickling (PoS) or the pO_2 at which the EI drops to 95% of the EI_{max} is denoted by filled circles in each group. EI_{min} is the lowest deformability that occurs when HbS polymerizes maximally at low pO_2. (D–F) The EI_{max}, EI_{min}, and pO_2 at PoS, respectively. Data in the deformability curves and oxygen-scan curves represent the mean deformability of all animals in that group: $n = 5$ mock SS mice, $n = 7$ GbG^{M} SS mice, and $n = 8$ GbG^{MI} SS mice. (D–F) Data are presented as mean ± SEM. One-way ANOVA. ns, not significant; $^{**}p < 0.01$, $^{***}p < 0.001$.

remarkably improved parameters when compared to mock mice (Figures 3C, 3D, and 3F). The PoS of RBCs in GbG^{M} and GbG^{MI} mice occurred at significantly lower pO_2 of 20.2 ± 3.4 and 18.7 ± 3.9 mmHg, respectively, when compared to a pO_2 of 38.7 ± 8.1 mmHg in mock mice (Figures 3C and 3F). Both EI_{min} and EI_{max} were significantly improved as well (Figures 3C–3E). C57 WT mice had no change in EI upon deoxygenation and reoxygenation as expected (uppermost curve in orange, Figure 3C). Thus, RBC functional parameters showed that both GbG^{M} and GbG^{MI} mice had significantly lower propensity to sickle and sickled only with extreme hypoxia with a minimal reduction in EI_{min} deformability compared to mock and had improved membrane deformability even during normoxia (EI_{max}) when compared to the mock RBCs.

Reduced extramedullary erythropoiesis, hemolysis, and improved survival

Spleen size is enlarged in sickle mice due to stress erythropoiesis and increased extravascular hemolysis.[35,36] There was approximately 50% reduction in spleen to body weight ratio in GbG^{M} mice and a 64% reduction in GbG^{MI} mice when compared to that in mock mice (Figure S2B), likely from reduced hemolysis, and reduced extramedullary hematopoiesis from the improved RBC health in both vector groups. SS recipient animals were followed up for 24 to 26 weeks post transplant where GbG^{M} and GbG^{MI} animals showed significantly improved survival (seven out of eight GbG^{M} survived; eight out of nine GbG^{MI} survived) when compared to mock animals (five out of eight animals survived) at 24 weeks post primary transplant.

High transduction efficiency in HSCs as seen in CFU-S in secondary transplanted mice

A secondary mouse CFU-S assay was performed to determine the proportion of GbG^{M} and GbG^{MI}-transduced cells. BM was collected from primary mice (1T) at 24 weeks and injected into eight secondary (2T) C57 WT recipients per group for obtaining CFU-S at 12 days post secondary transplant. Each colony was dissociated into a single-cell suspension and cells were divided for DNA isolation to determine VCN and for HbF staining to determine the percentage F cells in each colony. The percentage vector or HbF-positive CFU-S in 2T

Table 1. HSC transduction efficiency in CFU-S in 2T mice

1T mouse ID	Group	Total # of CFU-S isolated	Average VCN per CFU-S	% transduced CFU-S (based on VCN$^+$ colonies)	% transduced CFU-S (based on F cell$^+$ colonies)
1	G^bG^M	28	6.2	50	35.7
2		25	8.5	96	88
3		29	2.6	65.5	51.7
4		24	1.9	79.2	91.7
5		45	3.7	93.3	91.1
6		24	2.8	43.5	95.8
7		34	3.3	72.7	85.3
Average		**29.9**	**4.1**	**71.5**	**77.0**
8	G^bG^{MI}	36	2.2	41.7	44.4
9		29	3	86.2	75.9
10		39	3.8	56.8	46.2
11		20	3.1	60.6	20
12		35	2.7	40	88.6
13		25	4	40	92
14		38	2.8	81.6	100
15		33	1.7	60	33.3
Average		**31.9**	**2.9**	**58.4**	**62.6**

Eight 2T mice were transplanted with BM from one 1T mouse, and 3–5 CFU-S were isolated from each 2T mouse 12 days after the secondary transplant. The 1T animal from which the 2T CFU-S were derived are listed in column 1 and the total CFU-S isolated from all the 2T mice from that 1T mouse are listed in column 3. Half the CFU-S isolated was subjected to VCN analysis, and the other was half stained for HbF and subjected to flow cytometry. The HSC transduction efficiency in the 1T mice was calculated as the percentage of the number of CFU-S positive for vector copies divided by the total CFU-S isolated from the eight 2T mice transplanted from one 1T mouse or the percentage of the number of CFU-S positive for F cells (by FACS) divided by the total CFU-S isolated from all 2T mice transplanted from one 1T mouse. The percentage transduced CFU-S was thus calculated in two ways, based on VCN$^+$ CFU-S (column 5) or F cell$^+$ CFU-S (column 6): the threshold value to qualify F cell$^+$ colonies, >12% positive cells; the threshold value to qualify VCN$^+$ colonies, $\geq$0.4 copies per cell, to exclude contamination from surrounding splenic cells that get dissected along with the CFU-S. The percentage F cells and VCN in individual CFU-S in Figure S3.

mice represented the percentage of transduced cells that were engrafted in primary SS recipient mice. About 30 CFU-S in 2T mice transplanted from one 1T mouse were typically isolated. Secondary CFU-S data showed high percentage of transduced CFU-S in GbG^M mice (77% F cell-positive colonies and 71% VCN-positive colonies; Table 1). Similarly, the GbG^{MI} group had approximately 63% F cell-positive CFU-S and 58% VCN-positive CFU-S (Table 1). These data suggest that, on average, approximately 60%–70% of cells were efficiently transduced using GbG^M and GbG^{MI} vectors. The percentage F cells in individual 2T CFU-S obtained from all animals in GbG^M group ranged from 50% to 90% and 44% to 66% in the GbG^{MI} group (Figure S3A). The average VCN per 2T CFU-S in GbG^M mice was 4.1 and that in GbG^{MI} mice was 2.9 (Table 1; Figure S3B). Overall, the results of 2T CFU-S assay reflected the maintenance of long-term gene-modified HSPCs in the transplanted recipients.

Enhancer-blocking effects (reduced proto-oncogene activation) by GbG^M and GbG^{MI}

A genotoxicity assay was developed to assess the safety of GbG^M and the insulated GbG^{MI} LV. As a positive control, spleen focus-forming virus (SFFV) γ-RV vector, known to cause genotoxicity and activate proto-oncogenes such as LMO2,[37,38] was used in the assay. We identified a novel 36-bp foamy virus (FV)-derived insulator sequence with potent enhancer-blocking effects.[28] In order to test the ability of the strong LCR enhancer in the GbG^M provirus to activate LMO2, and the propensity of the Foamy insulator flanking the GbG^{MI} provirus to block the LMO2 activation, we knocked in the proviral forms of GbG^M, GbG^{MI}, and SFFV using clustered regularly interspaced short palindromic repeat (CRISPR) in HeLa cells (Figures S4A and S4B). The donor templates consisted of the proviral forms of the three vectors flanked by LMO2 homology arms. The GbG^M and GbG^{MI} donor plasmids contained a GFP expression cassette in addition, to allow selection of transfected cells. Since the SFFV RV expressed GFP driven by the SFFV promoter as a part of the proviral sequence, no additional GFP cassette was added to this plasmid (Figure S4A). The CRISPR-Cas9 plasmid had a BFP selection marker (Figure S4A). HeLa cells were transfected and dual BFP/GFP-expressing cells were sorted in bulk, expanded, and cloned as single cells, and about 6–12 clones confirmed molecularly to have precise targeted homology directed repair were allowed to proliferate for further analyses. Overall, approximately 1,425 total single-cell clones were derived, screened, and molecularly characterized to identify clones with correct gene targeting into LMO2 (Table S1). HeLa cells have four LMO2 alleles. The clones selected for LMO2 expression analyses showed similar median number of chromosomal alleles (a median of two alleles) targeted with the provirus with all three vectors, GbG^M, GbG^{MI}, and SFFV RV vectors (Figure S4C).

Next, we analyzed the LMO2 mRNA expression in targeted clones. Mock transfected/unedited HeLa cells have no LMO2 expression and therefore served as the negative control. The K562 cell line expresses very high levels of LMO2 and served as a positive control. LMO2 expression of clones with integrated SFFV, GbG^M, and GbG^{MI} proviruses showed a high upregulation of LMO2 by SFFV but no to minimal increase in LMO2 mRNA expression with GbG^M and almost no upregulation of LMO2 expression by the GbG^{MI} provirus. The difference in LMO2 expression between GbG^M and GbG^{MI} provirus clones was not statistically significant when multiple comparisons were done using ANOVA, albeit comparison only of GbGM and GbGMI using t test was significant ($p = 0.015$). Overall, we observed a highly significant decrease in LMO2 expression in both GbG^M and GbG^{MI} group when compared to the SFFV RV group (Figure 4A).

A western blot for LMO2 protein expression showed no expression in both GbG^M and GbG^{MI} bulk-sorted cells or clones, similar to unedited HeLa cells. Hence, at the protein level, we did not detect any LMO2 protein expression with either the GbG^M or GbG^{MI} vector. However, the samples in the SFFV RV group showed LMO2 protein expression (Figure 4B).

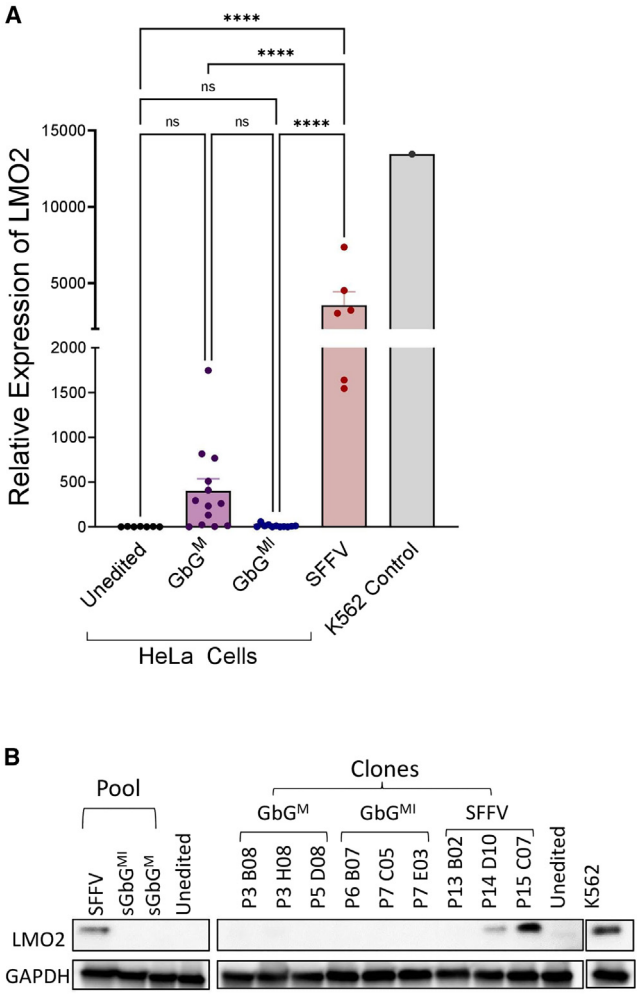

Figure 4. Expression of LMO2 following targeted integration of GbG^{M} and GbG^{MI} and SFFV provirus sequences

(A) LMO2 mRNA expression in individual HeLa cell clones confirmed to have targeted integration of the different provirus sequences. Unedited HeLa cell clones, which do not express LMO2, were the negative control, and K562 cells, known to express extremely high levels of LMO2, were the positive control. Each symbol represents an individual clones. Data presented as mean ± SEM. Statistics: one-way ANOVA. ns, not significant; ****$p < 0.0001$. (B) Western blot analysis of bulk-sorted edited HeLa cells, and three individual molecularly confirmed clones targeted with each of the three provirus sequences, probed for LMO2 protein expression. Since K562 cells expressed very high levels of LMO2 protein, a lower exposure of the gel.

In summary, we found both GbG^{M} and GbG^{MI} to be efficacious at correcting SCA. Both vectors carry erythroid specific enhancers and showed significantly reduced LMO2 proto-oncogene activation as compared to the SFFV RV LTR enhancer. The GbG^{MI} LV tended to have stronger enhancer-blocking effects than GbG^{M}; the differences, however, were not statistically significant between the two. Hence, we decided on GbG^{M} as the vector to be translated to a trial and performed further preclinical studies to demonstrate the safety of this vector. These studies have recently been published.[31] Since we previously reported rigorous safety analysis on a GbG^{M} vector surrogate (where the γ-globin gene was replaced by GFP and the vector backbone and promoter-enhancers were identical),[24] we did not pursue further safety studies using the in vitro immortalization (IVIM) assay. We did not perform IVIM assay or long-term safety of the GbG^{MI} vector in mice after the decision on the clinical vector was made.

Human CD34^{+} HSPCs transduced with GbG^{M} vector sustained long-term engraftment of gene-marked cells after xenotransplantation in NSG and NBSGW mice

To assess the ability of engraftment of human HSPCs transduced with GbG^{M} vector, we utilized human CD34^{+} cells isolated from adult mobilized peripheral blood (MPB) from a healthy donor as this source is relevant for gene-modified autologous transplantation rather than cord blood-derived HSPCs. Human MPB-derived CD34^{+} cells were transduced with GbG^{M} vector at an MOI of 50 and transplanted into NSG and NBSGW mice. As a control, we also transplanted untransduced MPB-derived human CD34^{+} cells with similar culture condition as the transduction group into sub-lethally irradiated NSG mice (mock). The GbG^{M}-transduced CD34^{+} cells were transplanted at varying cell doses into sub-lethally irradiated NSG mice (0.1e6, 0.5e6, and 1e6 cells/mouse; Figure 5A) and non-irradiated NBSGW mice (0.5e6 and 1e6; Figure 6A). Next, there was no difference of human cell engraftment observed in mock versus GbG^{M} NSG mice, showing lack of toxicity of the vector to HSPC and their engraftment (Figure 5B).

BM was analyzed at 20 weeks post transplantation. Dose response was observed; the level of human CD45^{+} cell engraftment in GbG^{M} NSG mice was significantly higher for the dose groups of 0.5e6 (57.3 ± 3.7, mean ± SEM) and 1.0e6 (51.3 ± 4.0) cell dose group when compared to 0.1e6 CD34^{+} lower cell dose group (22.6 ± 8.8) in all GbG^{M} mice (Figure 5A). In addition to human CD45^{+} cell engraftment, its differentiation into various lineages (representative fluorescence-activated cell sorting [FACS] shown in Figure S5) was also similar in all groups and comparable to mock mice in the BM, with similar proportion of human CD19^{+} B cells, CD33^{+} myeloid cells, CD3^{+} T cells, and CD34^{+} HSPCs (Figure 5C).

Similar results of a dose response and lineage output were seen in the spleen and thymus of the transplanted NSG mice. A dose-response increase of hCD45^{+} engraftment in the spleen of GbG^{M}-transduced mice was observed at increasing cell dose (Figure S6A), and multi-lineage distribution with higher proportion of B and T cells was observed in the spleen (Figure S6B). The VCN per cell analyzed in both spleen and thymus was similar to the VCN in BM except for the highest cell dose (1e6) group in the thymus (Figure S6C). The human CD45^{+} cell engraftment was highest in the thymus of the GbG^{M} mice as compared to BM and spleen with an average of 49%–72% of human cells being T cell population (Figures S6D and S6E).

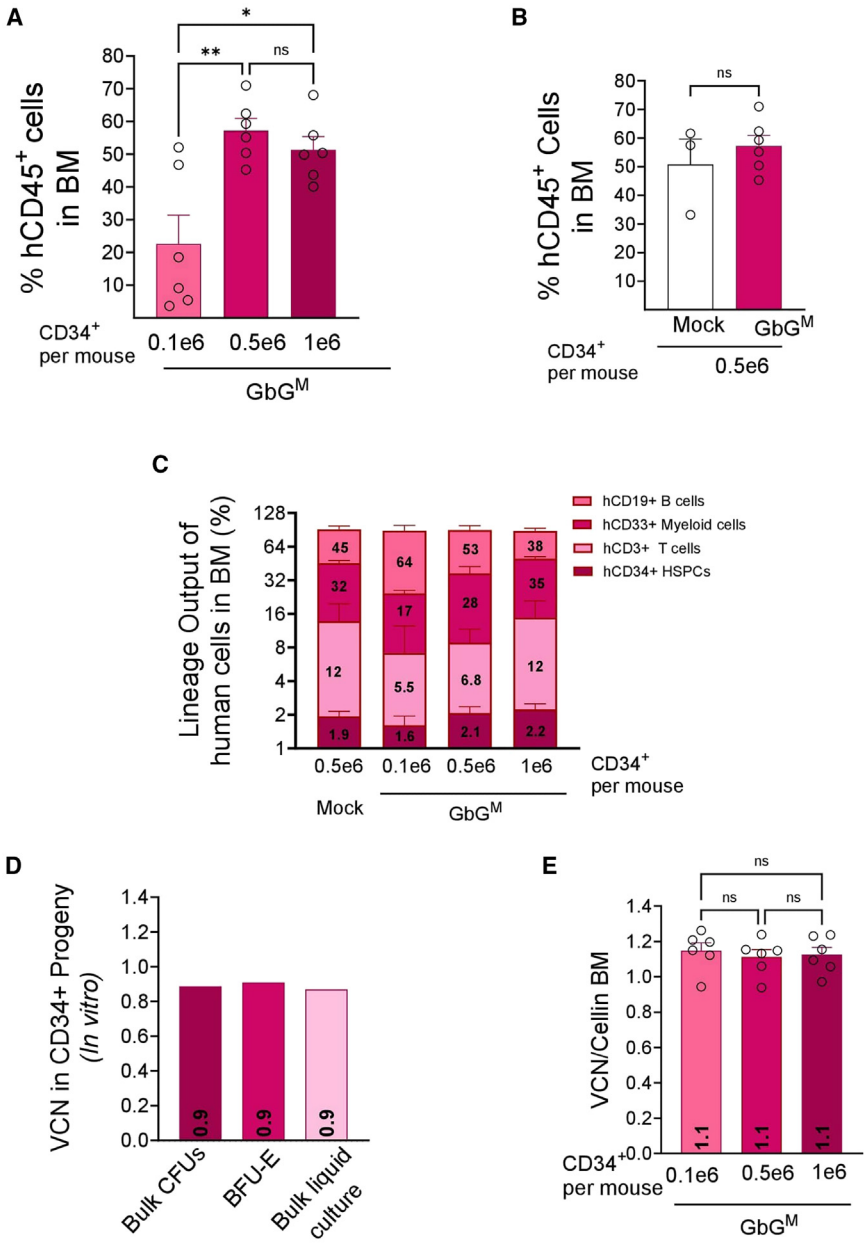

Figure 5. Engraftment of GbG^{M}-transduced human CD34^{+} HSPCs in NSG mice

(A) Engraftment of human CD34^{+} cells transduced with GbG^{M} Lentiviral vector (LV) or with no vector (mock) and transplanted into sub-lethally irradiated female NSG recipient mice at three different cell doses as indicated at 20 weeks. Engraftment was measured as human CD45^{+} (hCD45^{+}) cells in BM. (B) Comparative engraftment in NSG mice were injected with 0.5e6 mock and GbG^{M} CD34^{+} cells at 20 weeks. (C) Multi-lineage differentiation to lymphoid (B lymphoid [CD19^{+}], T lymphoid [CD3^{+}], myeloid (CD33^{+}) cells, and HSPCs (CD34^{+}) in BM of GbG^{M} and mock mice. (D) VCN determined in GbG^{M}-transduced human CD34^{+} cells expanded in culture for 14 days (bulk liquid culture) or in pooled/bulk colony-forming units (CFU) and burst-forming unit-erythroid (BFU-E) colonies collected from the colony forming assay. (E) VCN in BM 20 weeks post transplant of the indicated number of CD34^{+} cells. Each symbol represents an individual mouse. GbG^{M} n = 6 NSG mice and mock n = 3 NSG mice. Data are presented as mean ± SEM. Each symbol represents an individual mouse. Statistics: (A and E) one-way ANOVA, (B) unpaired Student's t tests. ns, not significant; $^{*}p < 0.05$; $^{**}p < 0.01$.

A small portion of GbG^{M}-transduced CD34^{+} cells were maintained in a bulk liquid culture and also plated as colony-forming unit cells (CFU-Cs) in methylcellulose medium for 2 weeks. *In vitro* gene transfer was assessed via qPCR on both bulk liquid culture and CFU-Cs, showing a similar VCN of 0.9 per cell (Figure 5D), which was similar to the VCN *in vivo* (an average of 1.1 VCN/cell in BM of all GbG^{M} mice across all cell dose group) (Figure 5E).

Similarly, analysis of human engraftment in the BM of non-irradiated NBSGW mice showed an average human CD45 chimerism ranging from an average of 48%–65% (higher engraftment with increasing CD34^{+} cell dose) with normal proportion of multi-lineages with predominant B cell and low T cell engraftment (Figures 6A and 6B). Human CD45 engraftment was also present at high levels in spleen of the GbG^{M}-transplanted animals and similar lineage distribution to that in BM (Figures S7A, S7B, 6A, and 6B). VCN analysis in BM of NBSGW mice showed an average VCN of 0.8–0.9 per cell and similar levels in spleen (Figures 6C and S7C), demonstrating an efficient transduction of human HSPCs and its maintenance *in vivo*. Finally, secondary transplant was performed to follow up for the long-term engraftment of transduced stem cells. A 12-week post-transplantation analysis in secondary NBSGW mouse BM revealed a long-term human CD45 engraftment with normal lineage distribution and sustained gene transfer *in vivo* with an average copy number of 0.8 per cell (Figures 6D and 6E), confirming high HSC gene transfer.

DISCUSSION

We have previously reported that a hybrid gene carrying the human γ-globin exons and β-globin non-coding elements and promoter in an LV, GbG, expresses high levels of HbF to correct SCA in SS mice.[23] We next modified the LV in the same GbG vector backbone by creating a G16D mutation (GbG^{M} vector) to alter the electrostatic property of γ-globin and therefore improve its ability to form the HbF tetramer. Comparisons of the two vectors indeed show that GbG^{M}

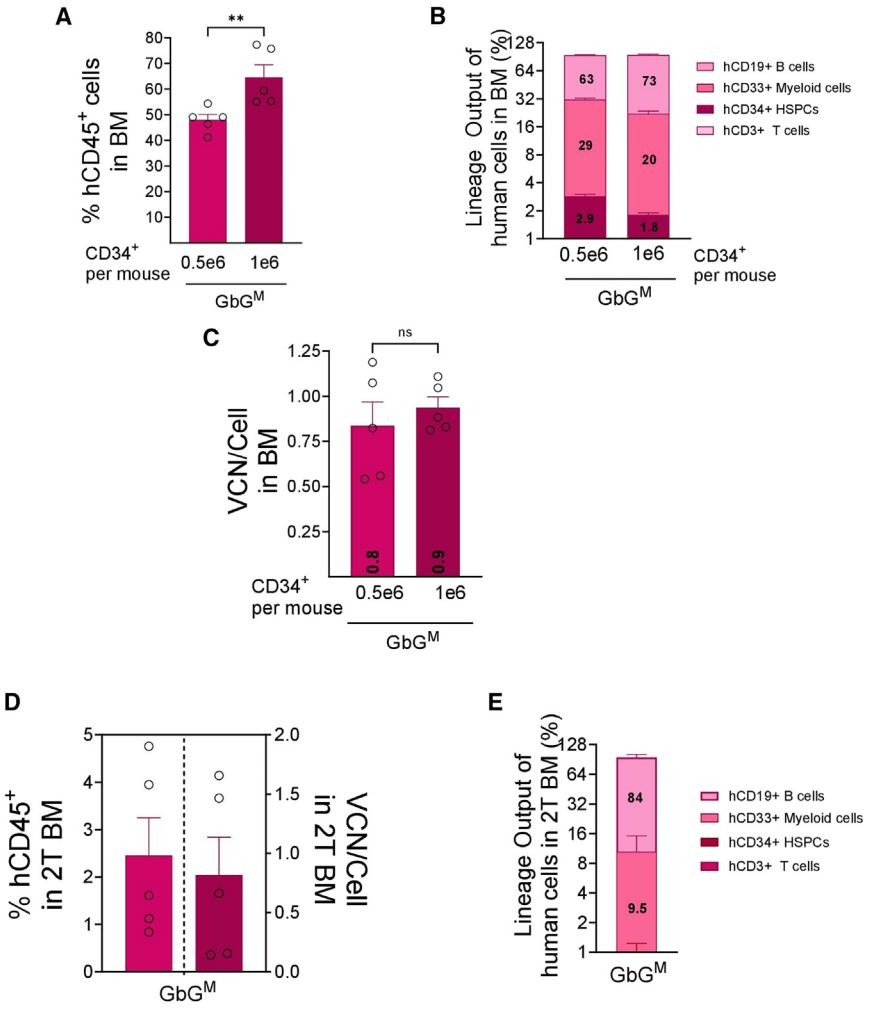

Figure 6. Engraftment of sGbG^{M} Lentiviralvector (LV)-transduced human CD34^{+} HSPCs in NBSGW mice

(A–C) MPB-derived human CD34^{+} cells transduced with sGbG^{M} LV were transplanted into five NBSGW primary recipient mice at two different doses as indicated. At 20 weeks, BM cells from the primary mice were analyzed for hematological reconstitution by flow cytometry. (A) Human CD45^{+} (hCD45^{+}) cell engraftment and (B) multi-lineage differentiation of lymphoid (B lymphoid [CD19^{+}], T lymphoid [CD3^{+}]), myeloid (CD33^{+}), and HSPCs (CD34^{+}) in GbG^{M} mice. (C) BM was analyzed to evaluate *in vivo* VCN in GbG^{M} mice at 20 weeks post transplant. Each symbol represents an individual mouse. n = 5 GbG^{M} NBSGW mice per cell dose. Data are presented as mean ± SEM. (A and C) Statistics: unpaired Student's t tests. ns, not significant; $^{**}p < 0.01$. (D and E) BM of primary transplanted GbG^{M} NBSGW mice (1e6 CD34^{+} cell dose group) at 20 weeks was transplanted into secondary NBSGW recipients (2T) for evaluating the long-term reconstitution of gene-modified stem cells. (D) Human CD45^{+} cell engraftment (left y axis) and VCN (right y axis) and (E) multi-lineage reconstitution in 2T NBSGW mice analyzed at 12 weeks post transplant. n = 5 GbG^{M} NBSGW 2T mice. Data are presented as mean ± SEM. Each symbol represents an individual mouse.

expresses 1.5- to 2-fold higher HbF/vector copy than GbG (data are being submitted as a separate study). In the preclinical studies presented herein, GbG^{M} is potent/efficacious at correcting SCA, with reduced intensity conditioning.

It becomes essential to have a consistent and more predictable expression of the therapeutic gene for achieving a long-term effect, especially for diseases where a higher proportion of gene-corrected HSCs and higher level of transgene expression are required. However, in the past, LV showed variable transgene expression and required a high number of vector copies per cell for a sustained therapeutic effect.[39] In order to address this, we had previously designed LVs flanked by the 1.2-kb chicken hypersensitive site-4 (cHS4) chromatin insulator element, which has both enhancer-blocking and barrier activity to protect from chromatin position effects. This resulted in higher human β-globin expression due to reduced position effects. However, despite the multiple advantages of cHS4 insulator, its large size significantly lowered vector titers and therefore was not clinically translatable. Later, we showed the mechanism of the reduction of titers by cHS4 was mainly due to the length of the insert in the 3′ LTR.[40] Attempts to use tandem copies of cHS4 insulator "core" sequences on both sides of the transgene cassette to improve the insulator activity resulted in lower titers and aberrant splicing into a cryptic splice site.[41] Moreover, two copies of insulator core elements added in the LV LTR showed retention of mostly a single copy in the provirus due to the recombination of the insulator sequences.[42] The insulator element (CCCTC) that binds the protein CTCF (CCCTC-binding factor) has enhancer-blocking properties.[43] We discovered a 36-bp CTCF-binding motif element in Foamy virus LTR that has potent enhancer-blocking effect.[28] Even though erythroid specific LCR enhancers in LV have shown safety in clinical trials of thalassemia and SCA, the LCR has low activity in HSPCs.[26] We therefore added a 36-bp enhancer-blocking FV insulator sequence in the 3′ LTR position to our GbG^{M} expression cassette to assess a proto-oncogene-activating potential of GbG^{M} and GbG^{MI}. Furthermore, the small size of this insulator sequence overcomes the common issue of insulator addition-mediated reduction in viral vector titers, which was indeed the case. When analyzed for enhancer-blocking effect by integrating the GbG^{M} and GbG^{MI} in the LMO2 proto-oncogene, both vectors had remarkably reduced activation of LMO2, with GbG^{MI} showing almost no activation. The difference between the GbG^{M}- and GbG^{MI}-mediated LMO2 mRNA expression was not statistically significant, though.

Both GbG^{M} and GbG^{MI} were transduced at similar MOI; however, an *in vitro* copy-number analysis revealed higher VCN in the GbG^{M} group when compared to GbG^{MI}, which is likely due to biological variability in transduction or slightly smaller size of GbG^{M} vector. The preclinical studies were done with one large preclinical batch of the two vectors. Although it is highly unlikely, a rigorous comparison with different vector preparations of both vectors is necessary to determine if the small 36-bp insulator sequence affects transduction efficiency. Nevertheless, a detailed analysis of transplantation of genetically modified HSCs into secondary mice showed that, in both the GbG^{M} and GbG^{MI} groups, the *in vitro* gene transfer into LSK HSPCs (which had a VCN of 4.8 and 3.3, respectively) was sustained at nearly 85% in the HSC assay in secondary mice (average VCN in secondary CFU-S was 4.1 and 2.9, respectively), even though the VCN in primary mice at 6 months appeared lower. When analyzed for anti-sickling globin HbF^{G16D} expression in both GbG^{M} and GbG^{MI} groups, approximately 36%–50% HbF was seen as early as 6 weeks post transplants and both groups of mice had nearly 40% HbF^{G16D} 6 months post primary transplant, with approximately 80%–90% F cells.

The GbG^{M} and GbG^{MI} animals had improved survival compared to mock animals. The one GbG^{M} mouse that died had similar VCN and percentage HbF to all the other GbG^{M} mice, and the histological analysis was inconclusive because of significant autolysis observed in the major organs due to death prior to sacrifice. Procedural mortality is common in SS mice and therefore the cause of death was likely due to this reason.

Both GbG^{M} and GbG^{MI} transduction significantly improved hematological indices in recipient sickle mice, including reduced anemia, reticulocytosis, and leukocytosis, which was evident in RBC functional assays: improved overall RBC deformability and the initiation of sickling of RBCs was significantly delayed at much lower oxygen concentrations when compared to mock animals. This is the first preclinical assessment of using Oxygenscan as a functional assay to study the correction of SCA disease phenotype by using modified gamma-globin carrying LV \. This analysis provides proof of concept to evaluate this technique as a functional assay in the clinic. Notably, GbG^{MI} mice, even with lower VCN than GbG^{M} mice, had almost similar levels of HbF^{G16D}, suggesting a higher probability of expression conceivably due to insulator-mediated decreased interference from repressive cellular sequences flanking the provirus. This result was also reflected in the secondary CFU-S.

Overall, both vectors were similarly efficacious. Our prior study using IVIM,[24] and *in vivo* studies in primary and secondary transplanted mice, showed markedly reduced genotoxicity with the GbG vector. This vector has an identical backbone to GbG^{M} and only differs from GbG^{M} by the G16D mutation in γ-globin. The clinical experience with similar uninsulated β-globin vector that has been used to treat over 50 patients with thalassemia and SCA has also shown vector safety. Based on this, we selected GbG^{M} as the vector to take forward into human preclinical and clinical studies. Additionally, we conducted a safety profile assessment study for this vector in healthy mice to support our IND submission.[31]

A large-scale transduction and transplant of human $CD34^{+}$ HSPC from MPB with the preclinical lot of GbG^{M} showed a VCN of 0.9–1, with 90% gene transfer based on CFU plated from the transduced $CD34^{+}$ cells *in vitro*. This VCN levels were retained and identical *in vivo*, both in NSG and NBSGW mice 20 weeks post transplant. Engraftment of $CD34^{+}$ cell was also dose dependent, with no toxicity or effect on the lineage output.

In summary, these preclinical studies in the sickle-to-sickle transplantation SS mouse model allowed a thorough comparison of the efficacy and safety of the GbG^{M} and the insulated GbG^{MI} vectors in mouse and human HSCs. Both vectors completely correct the sickle cell phenotype in SS mice, with insignificant differences in safety. The GbG^{M} LV resulted in high-level gene transfer into human HSCs and retention of the same VCN *in vivo* as was seen *in vitro* in two different types of immune-deficient mouse model 5 months post transplant and was chosen to be the vector that was translated to a phase I/II clinical trial (NCT 02186418). While the current data show no evidence of genotoxicity (even in primary and secondary transplants), more comprehensive studies would strengthen the safety profile over the long term. We acknowledge that late-stage malignancy risk, particularly in conditions like sickle cell disease (SCD), are still a valid concern, given what has been documented in clinical scenarios involving busulfan treatment[44] and the baseline risk of Acute Myeloid Leukemia (AML) in SCD patients.[45]

MATERIALS AND METHODS

Mice

SS mice[28] (ages ranging from 6 to 15 weeks; 16 females and eight males) were used for this study. SS mice are knockouts for mouse β^{major}- and α-globin genes and express human sickle hemoglobin (HbS) from human α- and β^{S}-globin from a transgene. The SS mouse pathology resembles severe human SCD. All animals in this study were bred and maintained in Cincinnati Children's Research Foundation's vivarium under Institutional Animal Care and Use Committee (IACUC)-approved protocols.

The immunocompromised NOD.Cg-Prkdc^{scid} Il2rg^{tm1Wjl}/SzJ (NSG) and NBSGW[29] mice were purchased from The Jackson Laboratory (USA). The study was conducted in compliance with the current version of the following: (1) Animal Welfare Act Regulations (9 CFR); (2) US Public Health Service Office of Laboratory Animal Welfare (OLAW) Policy on Humane Care and Use of Laboratory Animals; (3) Guide for the Care and Use of Laboratory Animals (Institute of Laboratory Animal Resources, Commission on Life Sciences, National Research Council, 1996); and (4) AAALAC accreditation.

LV design, titration, and murine HSPC transduction

The GbG^{M} vector is identical to the previously published GbG lentiviral vector (LV)[23] except for an additional point mutation in exon 1 that changes glycine (G) at the 16th position to aspartic acid (D),

generating HbF^{G16D} instead of HbF. The GbG^{MI} LV has the FV insulator (36-bp sequence) in the 3′ LTR. LV were produced by transient co-transfection of 293T cells (ATCC) as described previously.[28,46] The viral vectors were titered on mouse erythroleukemia (MEL) cells using serial dilutions and quantifying the HbF-expressing cells by flow cytometry, as previously described.[46]

Pilot studies (both *in vitro* and *in vivo*) were performed initially to optimize experiments and procedures for determining the efficacy of GbG^{M} and GbG^{MI} vectors in correcting the SCD phenotype in SS mice. Based on the pilot studies results, various assays were performed in this definitive transplant study to yield efficacy endpoints in primary and secondary mice. This experiment was designed to transplant 24 SS-recipient mice with BM derived from stem and progenitor cells ($Lineage^{-}$ $Sca1^{+}$ $cKit^{+}$: LSK cells) of 24 donor SS mice transduced with either mock (negative control) or with GbG^{M} or GbG^{MI} LV. BM was harvested from all four limbs of SS donor mice and the single-cell suspensions were prepared by dissecting all four limbs and pelvic bones (hind limbs consisted of femurs, tibias, and iliac crests) of all mice and crushing the bones in a mortar with sterile cold medium (Iscove's Modified Dulbecco's Medium supplemented with 2.0% FBS and 1% penicillin/streptomycin). BM mononuclear cells (MNCs) were isolated using Ficoll separation medium, stained with murine lineage antibody cocktail (against T cells, B cells, myeloid cells, and erythroid cells), and then the lineage-negative cells were obtained after magnetic lineage depletion procedure. After staining, the lineage-depleted cells were then sorted on a FACS ARIA for live LSK cells. The LSK cells were pre-stimulated for 2–4 h and transduced in StemSpan medium containing recombinant 10 ng/mL murine interleukin (IL)-3, 50 ng/mL murine Stem Cell Factor (SCF), and 25 ng/mL of murine Thrombopoietin (TPO) for all three groups (mock, GbG^{M}, and GbG^{MI}). An *in vitro* pilot study on LSK cells was conducted to decide on an optimal vector MOI (MOI of 25) that resulted in a high transduction efficiency without an overt toxicity. Twenty-two hours after transduction, the LSK cells from each group were harvested. Cells were then injected into 24 recipient SS mice (eight mice per group), with each mouse receiving approximately 46,000 LSK cells. After harvesting most (>95%) of the LSK cells from the wells for transplant, StemSpan medium with cytokines was added back into the wells to expand the remaining LSK cells for *in vitro* bulk culture VCN in the input cells. The LSK cells expanded *in vitro* were then harvested for VCN of input LSK cells at 14 days. DNA was extracted and a real-time PCR was run for VCN from each of the bulk cultures.

BM transplantation

On the day of transplant, primary recipient SS mice were sub-lethally irradiated with 875 cGy, split into two doses of 700 and 175 cGy, given approximately 3–4 h apart. LSK donor cells were harvested, washed once using 1× Dulbecco's phosphate-buffered saline (DPBS), centrifuged, and re-suspended in sterile cold 1× DPBS then intravenously (i.v.) injected into irradiated SS mouse tail vein. Each SS-recipient mouse received approximately 46,000 LSK cells, which were re-suspended in 200 μL of sterile 1× DPBS for injection via tail vein.

Following transplant, all mice were observed daily and weighed weekly. The observations were unremarkable except for an occasional eye swelling (resolved) and hair loss in a couple of mice. Animals had nominal weight fluctuations with no remarkable weight loss in the peri-transplant period. There were four animal deaths observed during the study (in three mock mice and one GbG^{M} mouse), which were likely related to the severity of SCD or to the procedural mortality in this model. Mice were bled at 6 weeks post transplant to determine the gene transfer and the success of the transplant via F cell analysis. Mice were then bled at 20 weeks post transplant to obtain a complete blood count (CBC), reticulocytes, HbF, F cell analysis, and VCN. Mice were considered evaluable if VCN was 0.5 or greater and analyzed further after 20 weeks. At 24–26 weeks, mice were sacrificed for organ evaluation and measurement of hematological parameters. BM processed after the sacrifice of evaluable primary animals was injected into eight secondary recipients per group for obtaining CFU-S.

Hematological assessment

Whole blood was obtained from SS mice from the retro-orbital sinus in EDTA tubes. A portion of the whole blood was subjected to CBC measurement using Hemavet 950FS (Drew Scientific, CT, USA) blood analyzer under mouse settings.

Reticulocyte analysis was performed using fresh or fixed blood. For fresh samples, 300 μL of Retic-COUNT reagent (BD Biosciences) and 1 μL of blood were mixed and incubated at room temperature for 30 min in the dark. For samples fixed with 4% paraformaldehyde (PFA), 250 μL of BD Retic-COUNT reagent, and 15 μL of PFA-fixed blood were mixed and incubated at room temperature for 1 h in the dark. Samples were analyzed by flow cytometry on FACS Canto 1 (BD Biosciences, San Jose, CA).

RBC functional analyses

RBC deformability was assessed using a laser-assisted optical rotational red cell analyzer (Lorrca, RR Mechatronics, the Netherlands) where the EI of RBCs was measured at increasing shear stress under ambient pO_2. RBC sickling characteristics were measured by subjecting RBCs to Lorrca with the Oxygenscan module 5. About 300–500 μL of whole EDTA blood samples were collected from SS-recipient mice at 24–26 weeks post primary transplant and about 40–50 μL of whole blood (containing 200 million RBCs) was utilized for Oxygenscan and ektacytometry.

VCN analysis

After extracting the genomic DNA either from lysed blood (WBCs) or from whole BM, a real-time qPCR was run to determine the VCN using primers and probes described previously.[6] In some samples, the VCN was determined by using digital droplet PCR (ddPCR). For qPCR, the R-U5 region was amplified, and, for ddPCR, the Psi region was amplified. Mouse ApoB was used as an endogenous control.

CZE for globin analysis

The percentage of therapeutic globin (HbF^{G16D}) in mouse blood samples was determined by CZE using RBC lysate (Capillarys 2, Sebia,

France) at Erythrocyte Diagnostic Laboratory (EDL), Comprehensive Mouse and Cancer Core (CCHMC).

Flow cytometry for F cells

Flow cytometry for human HbF was performed using fixed and permeabilized whole blood stained with anti-human Phycoerythrin (PE)-conjugated HbF antibody (Thermo Fisher Scientific, USA # MHFH04) per manufacturer's instructions.

Secondary transplant and CFU-S harvest

BM was processed after the sacrifice of primary animals (1T) (using both hindlimbs of each 1T mouse); 1×10^5 BM cells/mouse were injected into eight sub-lethally irradiated secondary C57BL/6 (WT) recipients (2T) per group for obtaining 30 CFU-S at 12 days post secondary transplant. The irradiation dose for 2T mice was 900 cGy split over 3–4 h with an initial dose of 700 cGy followed by a second dose of 200 cGy.

Human CD34$^+$ cell transduction and engraftment

Human MPB cells were purchased from AllCells and CD34$^+$ cells were isolated via CliniMacs device (Miltenyi Biotec, Auburn, CA, USA), cryopreserved, and then transduced with GbG^M vector at an MOI of 50 in Stromal Cell Growth Medium (SCGM) (CellGenix, Portsmouth, NH, USA) supplemented with human recombinant human SCF (rh-SCF, 300 ng/mL), rh-FLT3L (300 ng/mL), rh-TPO (100 ng/mL) (all cytokines from Peprotech, Cranbury, NJ, USA), and T707 (transduction enhancer) for 36–42 h. The harvested transduced human CD34$^+$ cells were cryopreserved and later thawed and transplanted via tail vein injection into sub-lethally irradiated (175 cGy for the whole-body radiation using an X-ray irradiator equipped with a parallel opposed dual X-ray source system [CIDX]) NSG mice at three different cell doses of 0.1e6, 0.5e6, and 1e6 viable CD34$^+$ cells and into non-irradiated NBSGW mice at 0.5e6 and 1e6 CD34$^+$ cell dose. Mice were observed daily, and body weight was measured weekly for the duration of the study (no change in body weight was observed among all groups). Mice were sacrificed at 20 weeks post transplantation and BM (from femurs, tibias, and pelvic bones), spleen, and thymus were collected, and single cell suspensions were prepared. Cells from all sources (BM, spleen, and thymus) were used for DNA extraction (Quick DNA/RNA miniprep plus kit [Zymo Research, #D7003, Irvine, CA, USA]) and VCN was analyzed via qPCR (for details, see "VCN analysis" section). Human CD45$^+$ cell engraftment and multi-lineage distribution was assessed by flow cytometry using the following antibodies: Brilliant Violet 421 anti-mouse CD45 antibody (#103134), APC anti-humanCD45 Antibody (#304037), anti-human hCD33-Phycoerythrin (PE) (#366608), anti-human hCD19-PE-Cy7 (#302216), anti-human hCD34-PerCP-Cy5.5 (#343522), and anti-human hCD3-FITC (#317306) (all antibodies were from BioLegend, San Diego, CA, USA). The sample acquisition was performed using MACSQuant 10 analyzer (Miltenyi Biotec, Auburn, CA). The flow cytometry results were analyzed using FlowJo software (version 10.8.1, Ashland, OR, USA). For secondary transplant, BM from primary mice (1e6 CD34$^+$ cell dose group only) was harvested, depleted of mouse CD45$^+$ cell using biotin rat anti-mouse CD45 (BD Biosciences, San Jose, CA, USA, catalog # 553078) and streptavidin Particles Plus (BD Biosciences, San Jose, CA, USA, catalog #557812), and transplanted into five non-irradiated secondary NBSGW recipients at 1:1 ratio via tail vein injection. At 12 weeks post transplant, 2T mice were analyzed for human CD45$^+$ cell engraftment and lineage distribution.

Statistical analyses

The one tailed Student's unpaired t test in GraphPad Prism version 9.3.0 (GraphPad software, La Jolla, CA, USA) was used to analyze comparisons between two groups. ANOVA was used for analyzing >2 samples. Values were expressed as mean ± SEM. A p value of <0.05 was considered statistically significant.

DATA AVAILABILITY

All of the data and materials will be available upon request.

ACKNOWLEDGMENTS

We thank Jeff Bailey, Victoria Summey (CCHMC), and Scarlett Ripberger for their assistance with mouse procedures; Theodosia Kalfa and Rose Fessler from CCHMC for technical assistance; with Lorrca Oxygenscan, Pang-Kuo Lo, and Swetha Tati from Noble life Sciences for performing xenograft experiments. We also thank the Research Flow Cytometry core at CCHMC, Cell Processing Core at CCHMC, and Viral Vector Core at CCHMC for their services. This work was funded by Innovation Fund Award (Malik) CCHMC and Aruvant Sciences, US Inc.

AUTHOR CONTRIBUTIONS

P.M. conceived the overall project. A.S. and M.S. conceived the human xenograft (HX) project. P.M. and A.S. designed and supervised SS experiments. D.M.P. designed and performed all the safety experiments testing LMO2 activation. A.S., M.S., and J.S. designed and supervised HX experiments. A.S., S.F., M.C., K.W., and O.T.G. performed the SS mouse efficacy experiments. A.S., P.M., and M.S. analyzed and interpreted the data. A.S. and P.M. wrote the manuscript. P.M., A.S., M.S., S.F., M.C., O.T.G., D.M.P., J.S., and K.W. read, edited, and approved the manuscript.

DECLARATION OF INTERESTS

The following authors were or are employees of Aruvant Sciences, Inc.: M.S., A.S., and J.S. P.M. holds patents with, and received royalties from, Aruvant Sciences and CSL Behring and has provided consultancy services to Aruvant Sciences.

SUPPLEMENTAL INFORMATION

Supplemental information can be found online at https://doi.org/10.1016/j.omtm.2025.101439.

REFERENCES

1. Rees, D.C., Williams, T.N., and Gladwin, M.T. (2010). Sickle-cell disease. Lancet *376*, 2018–2031.
2. Ingram, V.M. (1957). Gene mutations in human haemoglobin: the chemical difference between normal and sickle cell haemoglobin. Nature *180*, 326–328.
3. Bunn, H.F. (1997). Pathogenesis and treatment of sickle cell disease. N. Engl. J. Med. *337*, 762–769.
4. Padlan, E.A., and Love, W.E. (1985). Refined crystal structure of deoxyhemoglobin S. II. Molecular interactions in the crystal. J. Biol. Chem. *260*, 8280–8291.
5. Stamatoyannopoulos, G. (1972). The molecular basis of hemoglobin disease. Annu. Rev. Genet. *6*, 47–70.
6. Peterson, E.E., Salemi, J.L., Dongarwar, D., and Salihu, H.M. (2020). Acute care utilization in pediatric sickle cell disease and sickle cell trait in the USA: prevalence, temporal trends, and cost. Eur. J. Pediatr. *179*, 1701–1710.

7. Poletti, V., Urbinati, F., Charrier, S., Corre, G., Hollis, R.P., Campo Fernandez, B., Martin, S., Rothe, M., Schambach, A., Kohn, D.B., and Mavilio, F. (2018). Pre-clinical Development of a Lentiviral Vector Expressing the Anti-sickling βAS3 Globin for Gene Therapy for Sickle Cell Disease. Mol. Ther. Methods Clin. Dev. *11*, 167–179.

8. Italia, K., Jijina, F., Merchant, R., Swaminathan, S., Nadkarni, A., Gupta, M., Ghosh, K., and Colah, R. (2013). Comparison of in-vitro and in-vivo response to fetal hemoglobin production and γ-mRNA expression by hydroxyurea in Hemoglobinopathies. Indian J. Hum. Genet. *19*, 251–258.

9. Brodsky, R.A., and DeBaun, M.R. (2020). Are genetic approaches still needed to cure sickle cell disease? J. Clin. Investig. *130*, 7–9.

10. Leonard, A., Tisdale, J., and Abraham, A. (2020). Curative options for sickle cell disease: haploidentical stem cell transplantation or gene therapy? Br. J. Haematol. *189*, 408–423.

11. Naldini, L. (2015). Gene therapy returns to centre stage. Nature *526*, 351–360.

12. Goodman, M.A., and Malik, P. (2016). The potential of gene therapy approaches for the treatment of hemoglobinopathies: achievements and challenges. Ther. Adv. Hematol. *7*, 302–315.

13. Frangoul, H., Locatelli, F., Sharma, A., Bhatia, M., Mapara, M., Molinari, L., Wall, D., Liem, R.I., Telfer, P., Shah, A.J., et al. (2024). CLIMB SCD-121 Study Group. Exagamglogene Autotemcel for Severe Sickle Cell Disease. N. Engl. J. Med. *390*, 1649–1662.

14. Kanter, J., Walters, M.C., Krishnamurti, L., Mapara, M.Y., Kwiatkowski, J.L., Rifkin-Zenenberg, S., Aygun, B., Kasow, K.A., Pierciey, F.J., Jr., Bonner, M., et al. (2022). Biologic and Clinical Efficacy of LentiGlobin for Sickle Cell Disease. N. Engl. J. Med. *386*, 617–628.

15. Boulad, F., Maggio, A., Wang, X., Moi, P., Acuto, S., Kogel, F., Takpradit, C., Prockop, S., Mansilla-Soto, J., Cabriolu, A., et al. (2022). Lentiviral globin gene therapy with reduced-intensity conditioning in adults with beta-thalassemia: a phase 1 trial. Nat. Med. *28*, 63–70.

16. Esrick, E.B., Lehmann, L.E., Biffi, A., Achebe, M., Brendel, C., Ciuculescu, M.F., Daley, H., MacKinnon, B., Morris, E., Federico, A., et al. (2021). Post-Transcriptional Genetic Silencing of BCL11A to Treat Sickle Cell Disease. N. Engl. J. Med. *384*, 205–215.

17. Kohn, D.B., Booth, C., Kang, E.M., Pai, S.Y., Shaw, K.L., Santilli, G., Armant, M., Buckland, K.F., Choi, U., De Ravin, S.S., et al. (2020). Lentiviral gene therapy for X-linked chronic granulomatous disease. Nat. Med. *26*, 200–206.

18. Mamcarz, E., Zhou, S., Lockey, T., Abdelsamed, H., Cross, S.J., Kang, G., Ma, Z., Condori, J., Dowdy, J., Triplett, B., et al. (2019). Lentiviral Gene Therapy Combined with Low-Dose Busulfan in Infants with SCID-X1. N. Engl. J. Med. *380*, 1525–1534.

19. Aiuti, A., Biasco, L., Scaramuzza, S., Ferrua, F., Cicalese, M.P., Baricordi, C., Dionisio, F., Calabria, A., Giannelli, S., Castiello, M.C., et al. (2013). Lentiviral hematopoietic stem cell gene therapy in patients with Wiskott-Aldrich syndrome. Science *341*, 1233151.

20. Cavazzana-Calvo, M., Payen, E., Negre, O., Wang, G., Hehir, K., Fusil, F., Down, J., Denaro, M., Brady, T., Westerman, K., et al. (2010). Transfusion independence and HMGA2 activation after gene therapy of human beta-thalassaemia. Nature *467*, 318–322.

21. Cartier, N., Hacein-Bey-Abina, S., Bartholomae, C.C., Veres, G., Schmidt, M., Kutschera, I., Vidaud, M., Abel, U., Dal-Cortivo, L., Caccavelli, L., et al. (2009). Hematopoietic stem cell gene therapy with a lentiviral vector in X-linked adrenoleukodystrophy. Science *326*, 818–823.

22. (2021). First gene therapy for adrenoleukodystrophy. Nat. Biotechnol. *39*, 1319.

23. Perumbeti, A., Higashimoto, T., Urbinati, F., Franco, R., Meiselman, H.J., Witte, D., and Malik, P. (2009). A novel human gamma-globin gene vector for genetic correction of sickle cell anemia in a humanized sickle mouse model: critical determinants for successful correction. Blood *114*, 1174–1185.

24. Arumugam, P.I., Higashimoto, T., Urbinati, F., Modlich, U., Nestheide, S., Xia, P., Fox, C., Corsinotti, A., Baum, C., and Malik, P. (2009). Genotoxic potential of lineage-specific lentivirus vectors carrying the beta-globin locus control region. Mol. Ther. *17*, 1929–1937.

25. Cesana, D., Ranzani, M., Volpin, M., Bartholomae, C., Duros, C., Artus, A., Merella, S., Benedicenti, F., Sergi Sergi, L., Sanvito, F., et al. (2014). Uncovering and dissecting the genotoxicity of self-inactivating lentiviral vectors *in vivo*. Mol. Ther. *22*, 774–785.

26. Cabriolu, A., Odak, A., Zamparo, L., Yuan, H., Leslie, C.S., and Sadelain, M. (2022). Globin vector regulatory elements are active in early hematopoietic progenitor cells. Mol. Ther. *30*, 2199–2209.

27. Emery, D.W. (2011). The use of chromatin insulators to improve the expression and safety of integrating gene transfer vectors. Hum. Gene Ther. *22*, 761–774.

28. Goodman, M.A., Arumugam, P., Pillis, D.M., Loberg, A., Nasimuzzaman, M., Lynn, D., van der Loo, J.C.M., Dexheimer, P.J., Keddache, M., Bauer, T.R., Jr., et al. (2018). Foamy Virus Vector Carries a Strong Insulator in Its Long Terminal Repeat Which Reduces Its Genotoxic Potential. J. Virol. *92*, e01639-17.

29. Pászty, C. (1997). Transgenic and gene knock-out mouse models of sickle cell anemia and the thalassemias. Curr. Opin. Hematol. *4*, 88–93.

30. McIntosh, B.E., Brown, M.E., Duffin, B.M., Maufort, J.P., Vereide, D.T., Slukvin, I.I., and Thomson, J.A. (2015). Nonirradiated NOD, B6.SCID Il2rγ-/- Kit(W41/W41) (NBSGW) mice support multilineage engraftment of human hematopoietic cells. Stem Cell Rep. *4*, 171–180.

31. Shadid, M., Shrestha, A., and Malik, P. (2024). Preclinical safety assessment of modified gamma globin lentiviral vector-mediated autologous hematopoietic stem cell gene therapy for hemoglobinopathies. PLoS One *19*, e0306719.

32. Conran, N., and Belcher, J.D. (2018). Inflammation in sickle cell disease. Clin. Hemorheol. Microcirc. *68*, 263–299.

33. Rab, M.A.E., van Oirschot, B.A., Bos, J., Kanne, C.K., Sheehan, V.A., van Beers, E.J., and van Wijk, R. (2019). Characterization of Sickling During Controlled Automated Deoxygenation with Oxygen Gradient Ektacytometry. J. Vis. Exp. *153*.

34. Hoover, R., Rubin, R., Wise, G., and Warren, R. (1979). Adhesion of normal and sickle erythrocytes to endothelial monolayer cultures. Blood *54*, 872–876.

35. Manci, E.A., Hillery, C.A., Bodian, C.A., Zhang, Z.G., Lutty, G.A., and Coller, B.S. (2006). Pathology of Berkeley sickle cell mice: similarities and differences with human sickle cell disease. Blood *107*, 1651–1658.

36. Szczepanek, S.M., McNamara, J.T., Secor, E.R., Jr., Natarajan, P., Guernsey, L.A., Miller, L.A., Ballesteros, E., Jellison, E., Thrall, R.S., and Andemariam, B. (2012). Splenic morphological changes are accompanied by altered baseline immunity in a mouse model of sickle-cell disease. Am. J. Pathol. *181*, 1725–1734.

37. Braun, C.J., Boztug, K., Paruzynski, A., Witzel, M., Schwarzer, A., Rothe, M., Modlich, U., Beier, R., Göhring, G., Steinemann, D., et al. (2014). Gene therapy for Wiskott-Aldrich syndrome–long-term efficacy and genotoxicity. Sci. Transl. Med. *6*, 227ra33.

38. Hacein-Bey-Abina, S., von Kalle, C., Schmidt, M., McCormack, M.P., Wulffraat, N., Leboulch, P., Lim, A., Osborne, C.S., Pawliuk, R., Morillon, E., et al. (2003). LMO2-associated clonal T cell proliferation in two patients after gene therapy for SCID-X1. Science *302*, 415–419.

39. Imren, S., Payen, E., Westerman, K.A., Pawliuk, R., Fabry, M.E., Eaves, C.J., Cavilla, B., Wadsworth, L.D., Beuzard, Y., Bouhassira, E.E., et al. (2002). Permanent and panerythroid correction of murine beta thalassemia by multiple lentiviral integration in hematopoietic stem cells. Proc. Natl. Acad. Sci. USA *99*, 14380–14385.

40. Urbinati, F., Arumugam, P., Higashimoto, T., Perumbeti, A., Mitts, K., Xia, P., and Malik, P. (2009). Mechanism of reduction in titers from lentivirus vectors carrying large inserts in the 3'LTR. Mol. Ther. *17*, 1527–1536.

41. Nielsen, T.T., Jakobsson, J., Rosenqvist, N., and Lundberg, C. (2009). Incorporating double copies of a chromatin insulator into lentiviral vectors results in less viral integrants. BMC Biotechnol. *9*, 13.

42. Ronen, K., Negre, O., Roth, S., Colomb, C., Malani, N., Denaro, M., Brady, T., Fusil, F., Gillet-Legrand, B., Hehir, K., et al. (2011). Distribution of lentiviral vector integration sites in mice following therapeutic gene transfer to treat β-thalassemia. Mol. Ther. *19*, 1273–1286.

43. Liu, M., Maurano, M.T., Wang, H., Qi, H., Song, C.Z., Navas, P.A., Emery, D.W., Stamatoyannopoulos, J.A., and Stamatoyannopoulos, G. (2015). Genomic discovery of potent chromatin insulators for human gene therapy. Nat. Biotechnol. *33*, 198–203.

44. Goyal, S., Tisdale, J., Schmidt, M., Kanter, J., Jaroscak, J., Whitney, D., Bitter, H., Gregory, P.D., Parsons, G., Foos, M., et al. (2022). Acute myeloid leukemia case after gene therapy for sickle cell disease. N. Engl. J. Med. *386*, 138–147.

45. Brunson, A., Keegan, T.H.M., Bang, H., Mahajan, A., Paulukonis, S., and Wun, T. (2017). Increased risk of leukemia among sickle cell disease patients in California. Blood *130*, 1597–1599.

46. Puthenveetil, G., Scholes, J., Carbonell, D., Qureshi, N., Xia, P., Zeng, L., Li, S., Yu, Y., Hiti, A.L., Yee, J.K., and Malik, P. (2004). Successful correction of the human beta-thalassemia major phenotype using a lentiviral vector. Blood *104*, 3445–3453.